ARTICLES
PUBLISHED ONLINE: 17 APRIL 2011 | DOI: 10.1038/NGEO1118
nature geoscience

Departures from eustasy in Pliocene sea-level records

Maureen E. Raymo[1*†], Jerry X. Mitrovica[2†], Michael J. O'Leary[3], Robert M. DeConto[4] and Paul J. Hearty[5]

Proxy data suggest that atmospheric CO_2 levels during the middle of the Pliocene epoch (about 3 Myr ago) were similar to today, leading to the use of this interval as a potential analogue for future climate change. Estimates for mid-Pliocene sea levels range from 10 to 40 m above present, and a value of +25 m is often adopted in numerical climate model simulations. A eustatic change of such magnitude implies the complete deglaciation of the West Antarctic and Greenland ice sheets, and significant loss of mass in the East Antarctic ice sheet. However, the effects of glacial isostatic adjustments have not been accounted for in Pliocene sea-level reconstructions. Here we numerically model these effects on Pliocene shoreline features using a gravitationally self-consistent treatment of post-glacial sea-level change. We find that the predicted modern elevation of Pliocene shoreline features can deviate significantly from the eustatic signal, even in the absence of subsequent tectonically-driven movements of the Earth's surface. In our simulations, this non-eustatic sea-level change, at individual locations, is caused primarily by residual isostatic adjustments associated with late Pleistocene glaciation. We conclude that a combination of model results and field observations can help to better constrain sea level in the past, and hence lend insight into the stability of ice sheets under varying climate conditions.

The scientific community relies on the predictive capabilities of numerical climate models to assess likely future climate scenarios[1] and, to evaluate the performance of such models, they are often used to 'hindcast' documented climate changes of the past. The mid-Pliocene warm period (MPWP), ~3.3 and 2.9 Myr, continues to be the target of many such experiments[2–5]. Proxy data suggest that atmospheric CO_2 levels at that time were similar to today (between 350 and 450 ppmv; ref. 6) and that global mean temperature was elevated by as much as 2–3 °C with respect to modern[7]. However, whereas reconstructions of temperature and CO_2 are largely in agreement between investigators, estimates of sea level (SL) at that time are so varied as to preclude an accurate determination of the sensitivity of polar ice sheets to a modest global warming. This uncertainty is compounded by the fact that the most sophisticated ice sheet models predict only about +12 m of eustatic SL rise, primarily from loss of the Greenland Ice Sheet (GIS) and West Antarctic Ice Sheet (WAIS) under conditions of maximum orbital forcing and 400 ppmv CO_2 (ref. 8). This is significantly lower than the +25 m sea-level boundary condition assumed in most General Circulation Model (GCM) experiments. Are ice sheet models inaccurate? Or does the fault lie in interpretation of scant geologic data that suggest significantly higher ancient sea levels?

The most cited estimates of mid-Pliocene SL are based on field-mapping of palaeoshoreline deposits (Table 1). Such palaeoshorelines must be corrected for subsequent movement owing to local tectonics, any local sediment loading, dynamic topography owing to mantle convective flow[9], and glacial isostatic adjustment (GIA; ref. 10), where the latter refers to the response of the Earth to ice volume changes extending from the Pliocene through the Pleistocene glacial cycles and into the Holocene. Historically, only the first of these corrections has been made, whereas the third and fourth effects have either been ignored or assumed to depart negligibly from a simple eustatic SL change. Here, we show that GIA effects can, in certain geographic locations, be several times larger than eustatic SL changes associated with increasing polar ice volume. By mapping the predicted GIA signal, or 'fingerprint' of isostasy, we are able to identify those locations most likely to provide palaeo-SL estimates close to eustatic and those where SL proxies will require a substantial elevation correction for isostatic overprinting. We end with an evaluation of published shoreline elevations in light of these results.

GIA models and methodology

Our simulations are based on a canonical treatment of post-glacial SL change[10] modified to incorporate time-varying shorelines owing to local onlap or offlap of water, the growth and melting of grounded, marine-based ice sheets, the associated migration of water into or out of these marine settings, and the feedback into SL of contemporaneous perturbations in the Earth's rotation vector (see Supplementary Information; refs 11–13). Our SL software has been benchmarked against comparably accurate solvers[14,15] as well as applied to the investigation of SL evolution since the last interglacial[16]. Note that we use the geological definition of SL, namely the difference between the height of the sea surface equipotential and the solid surface (crust). Changes in SL can arise from perturbations in the height of either of these bounding surfaces.

The SL simulations require a model for the viscoelastic structure of the Earth. We adopt a 1D, self-gravitating, Maxwell viscoelastic Earth model with the density and elastic structure prescribed using the seismically determined model PREM (ref. 17). In addition, we

[1]Department of Earth Sciences, Boston University, 685 Commonwealth Avenue, Boston, Massachusetts 02215, USA, [2]Department of Earth and Planetary Sciences, Harvard University, 20 Oxford Street, Cambridge, Massachusetts 02138, USA, [3]School of Arts and Sciences, University of Notre Dame, Fremantle, Western Australia 6959, Australia, [4]Department of Geosciences, University of Massachusetts, Amherst, Massachusetts 01003, USA, [5]Department of Environmental Sciences, University of North Carolina, Wilmington, North Carolina 28403, USA. †These authors contributed equally to this work. *e-mail: raymo@bu.edu.

Table 1 | Sea-level estimates for MPWP and predicted modern elevation of a 14 m eustatic change using two viscosity models.

Study/site	Latitude (°)	Longitude (°)	SL est (m)	VM2 (m)	LM (m)	Indicator (rel. to SL)
Dowsett and Cronin[26]						
Orangeburg Scarp, NC/SC	34.79 N	79.66 W	35*	11.3	26.3	Scarp base (absolute)
Krantz[27]						
Moore House Formation, VA	37.22 N	76.91 W	15–20†	10.6	26.8	Mar. seds. (minimum)
Wardlaw and Quinn[28]						
Enewetak Atoll, Pacific	11.50 N	162.33 E	20–25*	13.0	12.1	Mar. seds. (minimum)
Kaufman and Brigham-Grette[25]						
Nome coastal plain, Alaska	64.55 N	165.39 W	60†	13.7	19.1	Scarp base (absolute)
James *et al.*[29]						
Roe Plain, W. Australia	31.91 S	127.04 E	~30†	9.3	7.9	Scarp base (absolute)

*Orangeburg Scarp elevation adjusted by −50 m to correct for post-depositional uplift. Enewetak Atoll estimate adjusted by +112 m to correct for post-depositional subsidence. †Authors discuss possibility of post-depositional uplift but do not quantify such effects.

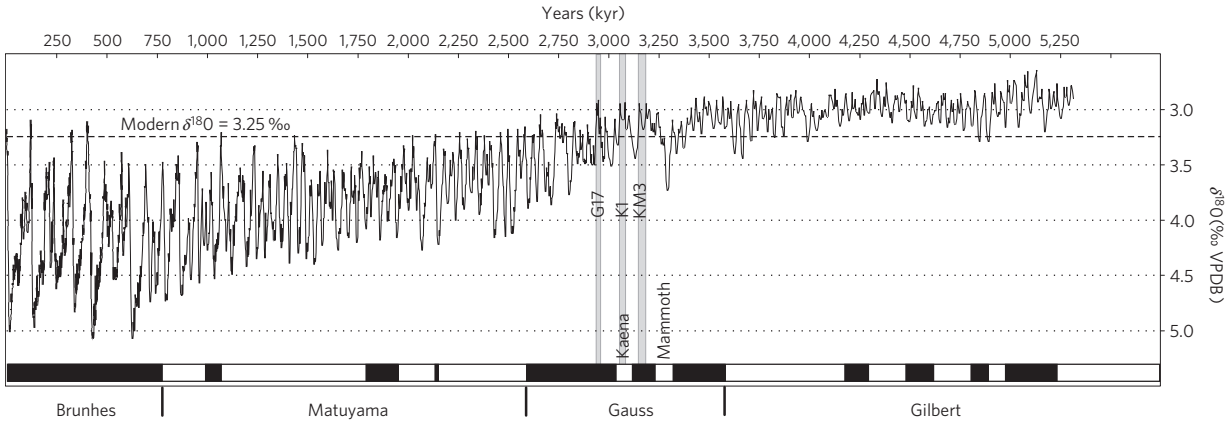

Figure 1 | Stack of globally distributed benthic $\delta^{18}O$ records[21] showing pattern of climate variability over past 5 Myr. The history of geomagnetic field reversals is shown on the lower *x* axis and labels G17, K1 and KM3 identify the three mid-Pliocene super-interglacials that fall within the MPWP.

investigate the SL response using two viscosity models; the first model (VM2) is characterized by an elastic lithosphere of 90 km thickness and a moderate viscosity increase from $\sim 5 \times 10^{20}$ Pa s in the upper mantle to $2–3 \times 10^{21}$ Pa s near the base of the mantle[18]. The second model (LM), representative of a broad class of viscosity models favoured by two independent groups[19,20], is characterized by an elastic lithospheric thickness of 120 km and a larger increase of viscosity with depth; from an upper mantle value of 5×10^{20} Pa s to a lower mantle value of 5×10^{21} Pa s.

In addition to an Earth model, an ice load history is needed to predict the geographic evolution of SL with time, in our case since the end of the MPWP to present-day. Our load history, similar (although not identical) to that predicted in the 400 ppmv CO_2 ice model experiment described earlier[8], is constructed in the following fashion. We assume, at 2.95 Myr, and for earlier times, a complete deglaciation of the WAIS and GIS and that the East Antarctic Ice Sheet (EAIS) thickness was at present-day values. After 2.95 Myr, we assume the WAIS and GIS increased rapidly to present-day thicknesses. From this time, the end of marine isotope stage (MIS) G17 (Fig. 1), until the peak of the last interglacial (MIS5e), ice volume is assumed to fluctuate according to a simple scaling of the LR04 benthic $\delta^{18}O$ stack and time scale[21] (Fig. 1). From MIS5e to the present-day, we use the ICE-5G history[18], and during earlier intervals we assume that the geographic variation of the ice cover for a specific ice volume/$\delta^{18}O$ value is the same as the ICE-5G cover for a similar ice volume. A sensitivity analysis related to the assumed ice history is discussed below. Note that a value of 12 m is often cited as the eustatic equivalent SL rise associated with melting of the polar ice sheets (7 m for the GIS (ref. 22) and 5 m for the WAIS (ref. 23)), an estimate that assumes the marine-based sectors of the grounded WAIS (the depressed holes left behind after the ice melts) would be filled with meltwater. However, in the experiments below we show that the predicted Pliocene eustatic equivalent SL change associated with these two ice sheets differs by 2 m from this value (it is 14 m). This is because our SL calculation predicts that the bedrock topography during the mid-Pliocene was higher than in the present-day West Antarctic region, an area now characterized by enhanced crustal depression owing to remnant loading effects from the last glacial cycle.

The GIA fingerprint on Pliocene sea-level markers

Using the above model and assumed ice load history (glaciation of an initially ice-free GIS and WAIS causing a 14 m eustatic equivalent SL fall), the SL algorithm[12] yields a prediction of the expected current height of a local marker of SL formed at 2.95 Myr, such as a coral reef, wave cut scarp or beach sequence (Fig. 2a). For example, along the southeast coast of the US, such a shoreline is predicted to now lie between 14 and 18 m above present SL and thus would over-estimate the eustatic SL fall at the end of the mid-Pliocene. Similarly, a marker of the MPWP highstand would be only ~3 m above SL at Tierra del Fuego, much lower than the actual eustatic fall. Departures from eustasy are even higher in previously glaciated regions. From this test we conclude that, even in the absence of local tectonic effects, the present elevation of mid-Pliocene highstands would not, in general, be an accurate, direct measure of past changes in ice volume.

The departure from eustasy is associated with the gravitational, deformational and rotational perturbations in the Earth system

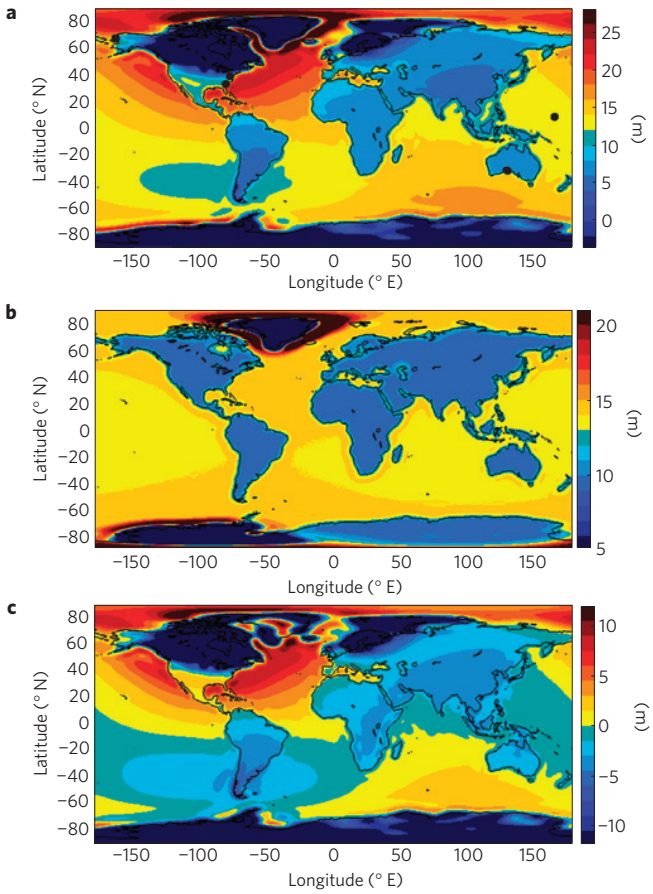

Figure 2 | Elevation (m), relative to modern SL, of a shoreline indicator deposited at 2.95 Myr predicted using the VM2 Earth model. a–c, In the assumed case of full deglaciation of the WAIS and GIS (**a**), the contribution to **a** from the initial ramp-up in ice volume at 2.95 Myr (**b**), the contribution to **a** from the residual disequilibrium associated with late Pleistocene ice and ocean loading (**c**). Frame **b** is computed as the difference between frames **a** and **c**. Dots represent locations of studies listed in Table 1. The SL change is plotted globally as the two bounding surfaces of SL, the sea surface and crustal height, are defined at all points on the surface. The water load only exists over the oceans, and the signal over land may be interpreted as the change in SL that would be measured if the site on land were connected to the ocean by an infinitesimally thin canal[31].

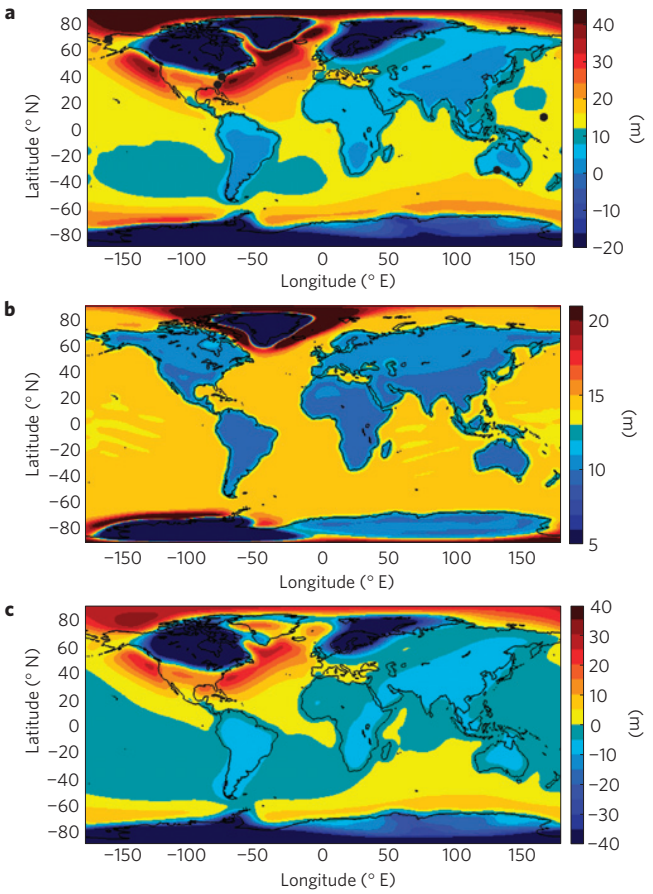

Figure 3 | Elevation (m), relative to modern SL, of a shoreline indicator deposited at 2.95 Myr predicted using the LM Earth model. a–c, In the assumed case of full deglaciation of the WAIS and GIS (**a**), the contribution to **a** from the initial ramp-up in ice volume at 2.95 Myr (**b**), the contribution to **a** from the residual disequilibrium associated with late Pleistocene ice and ocean loading (**c**). Frame **b** is computed as the difference between frames **a** and **c**. Dots represent locations of studies listed in Table 1.

driven by all loading that occurred between the time of the mid-Pliocene highstand and the present day. To understand the physical basis for this departure, it is useful to decompose the result in Fig. 2a into contributions associated with the modelled growth of the WAIS and GIS at 2.95 Myr (Fig. 2b) and the subsequent ice age cycles (Fig. 2c). In the millennia following the initial growth of ice in Greenland and the West Antarctic, the SL change associated with the ramp-up in ice volume would have been highly non-eustatic. However, as the ice and complementary ocean loads relaxed toward isostatic equilibrium, these departures diminish to decimetres or less, except in ocean regions close to Greenland and West Antarctica where the elastic lithosphere of the VM2 model prevents the Earth from ever reaching a state of perfect compensation, even after several million years (Fig. 2b). As the eustatic signal (~14 m) dominates in Fig. 2b, the prediction is relatively insensitive to both the detailed time history of ice volume changes leading up to 2.95 Myr (see Supplementary Information), as well as to the adopted profile of mantle viscosity (see below).

Whereas the response to the SL change that occurred during the MPWP has since relaxed to approximately eustatic, isostatic effects owing to loading by late Pleistocene ice sheets contribute a strong overprint to the expected current elavation of MPWP shorelines (Fig. 2c). This signal is, by definition, non-eustatic as we assume in our experiment that ice volume is the same during the initial post-MISG17 loading and at present (for example, growth of the WAIS and GIS to modern volumes). (Note that in practice a very small eustatic signal is associated with a change in the geometry of the shorelines across the post-MISG17 time window, and therefore, the size of the ocean basin, an adjustment our model takes into account.) Furthermore, the amplitude of the signal (Fig. 2c) has been decreasing since the start of the present interglacial as the Earth system evolves toward isostatic equilibrium following the last ice age cycle. The GIA overprint is not small; even outside areas of Pleistocene ice cover the amplitude of the signal can be of the same order as the eustatic signal that characterizes the assumed ice history.

The physics underlying the signals in Fig. 2c is well understood[24]. As an example, previously glaciated areas, such as Laurentia and Fennoscandia, are currently experiencing post-glacial uplift (at rates of ~1 cm yr^{-1}), and they are therefore far below their equilibrium SL position. Indeed, the predicted residual subsidence owing to the recent ice load amounts to order ~100 m using the ICE-5G history and the VM2 viscosity model; thus mid-Pliocene SL markers would still be many tens of metres below the eustatic level in these regions. Surrounding these regions of present-day uplift are the so-called peripheral bulges. These bulges, which include the coasts of North

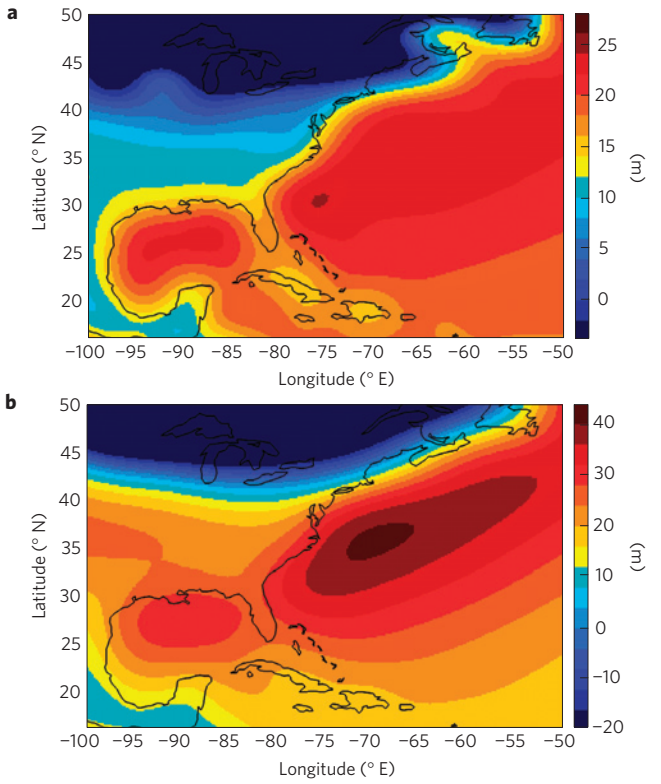

Figure 4 | Elevation (m) predictions for the east coast of the US and Mexico as in Figs 2a and 3a. a,**b**, Calculated using the VM2 model (**a**) and the LM model (**b**).

America, are presently subsiding (that is, SL is rising) at rates of several millimetre per year, and they are predicted to lie up to ~12 m above their equilibrium level in the ICE-5G/VM2 calculation (Fig. 2c). Finally, the low amplitude negative signal in the far-field of the late Pleistocene ice sheets indicates regions that are currently experiencing sub-millimetre per year SL fall owing to ocean syphoning effects[24]. In these zones, which include relatively low-latitude regions of the Pacific and Atlantic Oceans, ongoing GIA is dominated by a migration of water toward the subsiding peripheral bulges. The falling SL implies that these sites are currently below their equilibrium level, by as much as 4 m, and thus this residual depression would act to reduce the net height of mid-Pliocene SL markers from their eustatic level. Other effects, such as rotational feedback and continental levering[24], are also active in Fig. 2 and influence the detailed geometry of the signal, although to a lesser degree.

As in SL studies of the late Pleistocene, the signal owing to residual GIA (Fig. 2c) is highly sensitive to the ice history model used for the most recent deglaciation (see Supplementary Information) as well as to the adopted mantle viscosity structure. To explore the second of these sensitivities, we repeat the calculations using the LM viscosity profile instead of VM2 (Fig. 3). The SL perturbation owing to the ramp-up in model ice volume at ~3 Myr is very similar for both Earth models (Figs 2b and 3b); the difference, which is less than 0.20 m in the far field of the GIS and WAIS, is largely owing to the difference in the initial bedrock topography retrodicted by the two simulations. However, the higher viscosity of model LM relative to VM2 leads to a greater level of residual adjustment in response to the Pleistocene glacial cycles (compare Figs 3c and 2c, note scale change) with the net effect being a significantly larger perturbation to the present position of mid-Pliocene shorelines. For example, the peak elevation for a location off the southeast coast of the US is predicted to be ~42 m using model LM (Fig. 4b) but only ~24 m using model VM2 (Fig. 4a). Along the coastline south of Chesapeake Bay, for example,

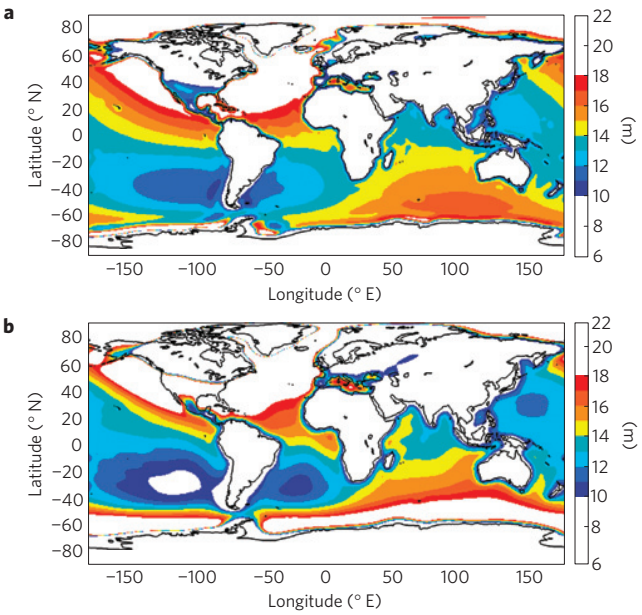

Figure 5 | Elevation (m), relative to modern SL, of a shoreline indicator deposited at 2.95 Myr, highlighting those regions where palaeoshorelines would lie within ±4 m of the predicted eustatic SL, as in Figs 2a and 3a. a,**b**, Calculated using the VM2 model (**a**), and the LM model (**b**).

the predicted elevation of a palaeoshoreline consistent with a +14 m eustatic SL change ranges from 14–18 m for the VM2 run and 24–34 m for the calculation based on model LM.

Implications for Pliocene sea level

We conclude that the present elevation of a fossil coral reef, geomorphic feature, or beach sequence laid down during a mid-Pliocene super-interglacial is controlled by two main factors (in the absence of subsequent tectonic or dynamic topography effects): (1) an approximately eustatic signal associated with the change in the baseline ice volume during the climate optimum (that is, before ~3 Myr) relative to today, a signal that is relatively insensitive to details regarding the assumed Earth model and mantle viscosity; and (2) a residual adjustment associated with the last glacial cycle of the ice age that is very sensitive to the adopted mantle viscosity profile. In regard to factor (1), our modelled ice history assumed a eustatic fall of ~14 m at the end of the MPWP owing to glaciation of the WAIS and GIS; but what if the MPWP was in fact characterized by much higher SL (and much smaller EAIS)? How would this alter model predictions of where Pliocene shoreline features would be found today? The main effect on these predictions would be an increase in the eustatic SL contribution; if the EAIS grew by the equivalent of 10 m of eustatic SL (to today's volume) at the end of the MPWP then, outside the EAIS region, the predictions in Figs 2b and 3b (and summed predictions in 2a and 3a) would be altered by the addition of this amount. Similarly, if the WAIS or GIS remained partially glaciated during the warm extremes of the mid-Pliocene, perhaps characterized by about half their present-day volume, then the eustatic signal in Figs 2b and 3b would be reduced by about half (to ~7 m), and the predicted elevation of mid-Pliocene shorelines (for example, in Figs 2a or 3a) would similarly decrease.

Thus, a template begins to emerge for targeted collection and analysis of observational data. In Fig. 5 we plot only those regions (in Figs 2a and 3a) where an identified palaeoshoreline would lie within ±4 m of the predicted eustatic SL value. As expected, these regions are primarily in the far-field of the late Pleistocene ice centres. Additionally, we see that along many coastlines palaeoshoreline features would typically be found a few metres below their actual eustatic elevation. This is primarily because of the combined effects

of ocean loading during the last deglaciation, whereby meltwater entering the ocean causes subsidence of regions offshore of continents and uplift of the continents, and ocean unloading owing to the ramp-up of ice volume at the end of the MPWP (see Figs 2 or 3).

The implications of our results for mid-Pliocene ice volume are highlighted by comparing predicted shoreline elevations (from two Earth/viscosity models) to available observations (Table 1). Five studies document a clear sedimentological or geomorphologic indicator of SL during the MPWP (for example, a feature that formed within metres of SL); these sites include northwestern Alaska[25], Orangeburg Scarp of North Carolina (corrected for local uplift[26]), Moore House Formation in Virginia[27], Enewetak Atoll in the Marshall Islands (corrected for subsidence[28]), and Roe Plain in Western Australia[29]. If one uses model VM2 and compares the elevation of the field data with the predicted modern elevation (at that site) of a Pliocene shoreline formed just before a 14 m eustatic SL fall (Table 1), then the field data that are corrected for local tectonic and subsidence effects[26,28] suggest an additional eustatic SL fall of 10–25 m may have occurred, implying melting of the EAIS during the MPWP. Alternatively, if one adopts model LM, then field observations from the Orangeburg Scarp suggest less of a change in EAIS volume ($<$10 m); and in this case, the predicted elevation for Enewetak Atoll is also about 10 m below what field observations suggest, still leaving room for substantial melting of the EAIS. In addition to ignoring poorly constrained errors in the uplift corrections, these inferences also assume no additional dynamic topography effects, which, in the case of the eastern US seaboard at least, seems unlikely[9]. In the case of Roe Plain (8–9 m predicted by both models), the observed $>$25 m elevation of palaeoshoreline features is likely caused by post-depositional uplift owing to dynamic topography[30].

The arguments above are intended as illustrations of the pitfalls and non-uniqueness of conclusions that do not account for glacioisostasy and its sensitivity to uncertainties in mantle viscosity. A rigorous analysis would not only require more data but would also take into account other confounding signals, such as steric effects and dynamic topography owing to mantle flow[9,30]. Ultimately, much needed constraints on Pliocene SL, and therefore ice volume, can only be achieved with a large global matrix of palaeoshoreline data, which does not yet exist, evaluated within the context of model predictions, or 'fingerprints', such as presented here. Indeed, results described here can be used to target diagnostic regions where evidence for palaeoshorelines should be sought.

Received 18 October 2010; accepted 22 February 2011; published online 17 April 2011

References

1. Intergovernmental Panel on Climate Change *Fourth Assessment Report* available at: http://www.ipcc.ch/ipccreports/ar4-syr.htm (2007).
2. Haywood, A. M., Valdes, P. J. & Sellwood, B. W. Global scale palaeoclimate reconstruction of the middle Pliocene climate using the UKMO GCM: Initial results. *Glob. Planet. Change* **25,** 239–256 (2000).
3. Haywood, A. M. & Valdes, P. J. Modelling Middle Pliocene warmth: Contribution of atmosphere, oceans and cryosphere. *Earth Planet. Sci. Lett.* **218,** 363–377 (2004).
4. Chandler, M., Rind, D. & Thompson, R. Joint investigations of the Middle Pliocene climate II: GISS GCM Northern Hemisphere results. *Glob. Planet. Change* **9,** 197–219 (1994).
5. Sloan, L. C., Crowley, T. J. & Pollard, D. Modelling of Middle Pliocene climate with the NCAR GENESIS general circulation model. *Mar. Micropaleontol.* **27,** 51–61 (1996).
6. Pagani, M., Liu, Z., LaRiveire, J. & Ravelo, A. C. High Earth-system climate sensitivity determined from Pliocene carbon dioxide concentrations. *Nature Geosci.* **3,** 27–30 (2010).
7. Dowsett, H. J. in *Deep-time Perspectives on Climate Change: Marrying the Signal from Computer Models and Biological Proxies* (eds Williams, M., Haywood, A. M., Gregory, J. & Schmidt, D.) 459–480 (The Micropalaeontological Society Special Publications The Geological Society of London, 2007).
8. Pollard, D. & De Conto, R. M. Modelling West Antarctic ice sheet growth and collapse through the past five million years. *Nature* **458,** 329–332 (2009).
9. Moucha, R., Forte, A. M., Mitrovica, J. X., Rowley, D. B & Quéré, S. Dynamic topography and long-term sea-level variations: There is no such thing as a stable continental platform. *Earth Planet. Sci. Lett.* **271,** 101–108 (2008).
10. Farrell, W. E. & Clark, J. A. On postglacial sea level. *Geophys. J. R. Astron. Soc.* **46,** 647–667 (1976).
11. Mitrovica, J. X. & Milne, G. A. On post-glacial sea level. I. General theory. *Geophys. J. Int.* **154,** 253–267 (2003).
12. Kendall, R. A., Mitrovica, J. X. & Milne, G. A. On post-glacial sea level: II. Numerical formulation and comparative results on spherically symmetric models. *Geophys. J. Int.* **161,** 679–706 (2005).
13. Mitrovica, J. X., Wahr, J., Matsuyama, I. & Paulson, A. The rotational stability of an ice age Earth. *Geophys. J. Int.* **161,** 491–506 (2005).
14. Mitrovica, J. X. Recent controversies in predicting post-glacial sea-level change: A viewpoint. *Quat. Sci. Rev.* **22,** 127–133 (2003).
15. Lambeck, K. & Chappell, J. Sea level change through the last glacial cycle. *Science* **292,** 679–686 (2001).
16. Kopp, R. E., Frederik, S. J., Mitrovica, J. X., Maloof, A. C. & Oppenheimer, M. Probabilistic assessment of sea level during the last interglacial stage. *Nature* **462,** 863–868 (2009).
17. Dziewonski, A. M. & Anderson, D. L. Preliminary reference Earth model (PREM). *Phys. Earth Planet. Int.* **25,** 297–356 (1981).
18. Peltier, W. R. Global glacial isostasy and the surface of the ice-age Earth: The ICE-5G (VM2) model and GRACE. *Annu. Rev. Earth Planet. Sci.* **32,** 111–149 (2004).
19. Lambeck, K., Smither, C. & Johnston, P. Sea-level change, glacial rebound and mantle viscosity for northern Europe. *Geophys. J. Int.* **134,** 102–144 (1998).
20. Mitrovica, J. X. & Forte, A. M. A new inference of mantle viscosity based on a joint inversion of convection and glacial isostatic adjustment data. *Earth Planet. Sci. Lett.* **225,** 177–189 (2004).
21. Lisiecki, L. E. & Raymo, M. E. A Pliocene–Pleistocene stack of 57 globally distributed benthic δ^{18}O records. *Paleoceanography* **20,** PA1003 (2005).
22. Bamber, J. L., Layberry, R. L. & Gogineni, S. P. A new ice thickness and bed data set for the Greenland ice sheet; 1. Measurement, data reduction, and errors. *J. Geophys. Res.* **106,** 33773–33780 (2001).
23. Lythe, M. B. & Vaughan, D. G. The BEDMAP Consortium, BEDMAP: A new ice thickness and subglacial topographic model of Antarctica. *J. Geophys. Res.* **106,** 11335–11351 (2001).
24. Mitrovica, J. X. & Milne, G. A. On the origin of postglacial ocean syphoning. *Quat. Sci. Rev.* **21,** 2179–2190 (2002).
25. Kaufman, D. S. & Brigham-Grette, J. Aminostratigraphic correlations and paleotemperature implications, Pliocene–Pleistocene high-sea-level deposits, northwestern Alaska. *Quat. Sci. Rev.* **12,** 21–33 (1993).
26. Dowsett, H. J. & Cronin, T. M. High eustatic sea level during the middle Pliocene: Evidence from the southeastern US Atlantic Coastal Plain. *Geology* **18,** 435–438 (1990).
27. Krantz, D. E. A chronology of Pliocene sea-level fluctuations: The US Middle Atlantic coastal plain record. *Quat. Sci. Rev.* **10,** 163–174 (1991).
28. Wardlaw, B. R. & Quinn, T. M. The record of Pliocene sea-level change at Enewetak Atoll. *Quat. Sci. Rev.* **10,** 247–258 (1991).
29. James, N. P., Bone, Y., Carter, R. M. & Murray-Wallace, C. V. Origin of the late Neogene Roe Plains and their calcarenite veneer: Implications for sedimentology and tectonics in the Great Australian Bight. *Aust. J. Earth Sci.* **53,** 407–419 (2006).
30. Sandiford, M. & Quigley, M. TOPO-OZ: Insights into the various modes of intraplate deformation in the Australian continent. *Tectonophysics* **474,** 405–416 (2009).
31. Dahlen, F. A. The passive influence of the oceans on the rotation of the Earth. *Geophys. J. R. Astron. Soc.* **46,** 363–406 (1976).

Acknowledgements

Support for this research was provided by NSF-OCE0825293 to M.E.R. and by Harvard University and The Canadian Institute for Advanced Research to J.X.M. We thank T. Cronin and J. Brigham-Grette for discussions of field data and support from the USGS PRISM program that helped jump-start this investigation.

Author contributions

M.E.R. and J.X.M. jointly conceived and designed the GIA model experiments and wrote first draft of paper; J.X.M. carried out the GIA experiments; R.M.D. provided ice sheet simulations; M.J.O. and P.J.H. contributed to analysis of geologic data; all authors contributed to discussions and revisions of the manuscript.

Additional information

The authors declare no competing financial interests. Supplementary information accompanies this paper on www.nature.com/naturegeoscience. Reprints and permissions information is available online at http://npg.nature.com/reprintsandpermissions. Correspondence and requests for materials should be addressed to M.E.R.